

Finite Element Analysis of Fully Developed Free Convection Flow Heat and Mass Transfer of a MHD / Micropolar Fluid over a Vertical Channel

Bala Siddulu Malga^{*,a}, Naikoti Kishan^b, V.V Reddy^c, K. Govardhan^a

^aDepartment of Mathematics, GITAM University, Hyderabad, Telangana, India.

^bDepartment of Mathematics, University College of Science, O.U, Hyderabad, Telangana, India.

^cDepartment of Mathematics, Kamala Nehru Polytechnic College, Hyderabad, Telangana.

Received 25 Dec 2012

Accepted 1 Aug 2014

Abstract

The present study analyzes the problem of the fully developed natural convection magneto-hydrodynamics micropolar fluid flow of heat and mass transfer in a vertical channel. Asymmetric temperature and convection boundary conditions are applied to the walls of the channel. The cases of double diffusion and Soret-induced connections are both considered. Solutions of the coupled non-linear governing equations are obtained for different values of the buoyancy ratio and various material parameters of the micropolar fluid and magnetic parameters, viscous dissipation. The resulting non-dimensional boundary value problem is solved by the Galerkin Finite element method using MATLAB Software. The influence of the governing parameters on the fluid flow as well as heat and solute transfers is demonstrated as significant.

© 2014 Jordan Journal of Mechanical and Industrial Engineering. All rights reserved

Keywords: : Finite Element Method, Natural Convection, Micropolar Fluid, Vertical Channel, Double Diffusion, Soret Effect, Viscous Dissipation, Skin Friction Coefficient, Nusselt Number

Nomenclature

B	micro-inertia parameter
g	gravitational acceleration
Gr	grashof number
H'	distance between the plates
j	micro inertia per unit mass
K	vortex viscosity parameter
M	magnetic Parameter
N	dimensionless angular velocity
n	dimensionless micro-gyration parameter
R_T	wall temperature
R_S	wall concentration
Ec	Eckert number
Nu	Nusselt Number
C_f	Skin friction coefficient

Greek symbols

μ	dynamic viscosity
φ	buoyancy ratio
ρ	density of fluid

γ spin-gradient viscosity

κ vortex viscosity

Subscripts

S	dimensionless Concentration
T	dimensionless temperature
u	dimensionless velocity in x direction
x	dimensionless coordinate axis
y	dimensionless coordinate axis
0	reference state
c	refers to critical conditions

Superscript

' refers to dimensional variable

1. Introduction

The micropolar fluid model introduced by Eringen [1] exhibits some microscopic effects arising from the local structure and micro motion of the fluid elements. Further, the micropolar fluid can sustain couple stresses and include classical Newtonian fluid as a special case. The model of micropolar fluid represents fluids consisting of

* Corresponding author. email: balumalga@gmail.com

rigid, randomly oriented (or spherical) particles suspended in a viscous medium where the deformation of the particles is ignored. Micropolar fluids have been shown to accurately simulate the flow characteristics of polymeric additives, geomorphological sediments, colloidal suspensions, hematological suspensions, liquid crystals, lubricants, etc. The theory of micropolar fluids, introduced by Eringen [2; 3] in order to deal with the characteristics of fluids with suspended particles, has received a considerable interest in recent years. Also, as demonstrated by Papautsky *et al.* [4], Eringen's model successfully predicts the characteristics of flow in microchannels. An excellent review of the various applications of micropolar fluid mechanics was presented by Ariman *et al.* [5]. The mathematical theory of equations of micropolar fluids and the applications of these fluids in the theory of lubrication and porous media are presented by Lukaszewicz [6]. The heat and mass transfer in micropolar fluids is also important in the context of chemical engineering, aerospace engineering and also industrial manufacturing processes.

The first study of the fully developed free convection of a micropolar fluid in a vertical channel was presented by Chamkha *et al.* [7]. This problem was extended by Kumar *et al.* [8] to consider the case of a channel with one region filled with micropolar fluid and the other region with a Newtonian fluid. It was found that the effects of the micropolar fluid material parameters suppress the fluid velocity but enhance the microrotation velocity. An analytical solution predicting the characteristics of fluid flow as well as heat and mass transfer was derived. It was reported that an increase of the vortex viscosity parameter tends to decrease the fluid velocity in the vertical channel. The same problem was later reconsidered by Bataineh *et al.* [9]. The problem of the fully developed natural convection heat and mass transfer of a micropolar fluid between porous vertical plates with asymmetric wall temperatures and concentrations was investigated by Abdulaziz *et al.* [10]. However, it is well known that convection, in a binary mixture, can also be induced by Soret effects. For this situation the species gradients result from the imposition of a temperature gradient in an otherwise uniform-concentration mixture. Two kinds of problems have been considered in the literature concerning the convection of a binary mixture filling a horizontal porous layer. The first kind of problems, called double diffusion, considers flows induced by the buoyancy forces resulting from the imposition of both thermal and solutal boundary conditions on the layer. Early investigations on double-diffusive natural convection in porous media primarily focused on the problem of convective instability in a horizontal layer (Nield [11], Taunton *et al.* [12], Poulikakos [13]).

The second kind of problems considers thermal convection in a binary fluid driven by Soret effects. For this situation the species gradients are not due to the imposition of solutal boundary conditions as in the case of double diffusion. Rather, they result from the imposition of a temperature gradient in an otherwise uniform-concentration mixture. Brand and Steinberg [14; 15] investigated the influence of Soret-induced solutal buoyancy forces on the convective instability of a fluid mixture in a porous medium heated isothermally. The first

study of Soret-induced convection was described by Bergman *et al.* [16], while considering natural convection in a cavity filled with a binary fluid. This flow configuration has also been investigated by R. Krishnan *et al.* [17]. As pointed out recently by Rawat *et al.* [18], the study of heat and mass transfer in micropolar fluids is of importance in the fields of chemical engineering, aerospace engineering and also industrial manufacturing effects processes. Sunil *et al.* [19] studied the effect of rotation on double-diffusive convection in a magnetized ferro fluid with internal angular momentum; A. A. Bakr *et al.* [20] studied the double-diffusive convection-radiation interaction on unsteady MHD micropolar fluid flow over a vertical moving porous plate with heat generation and Soret effects. R. A. Mohamed [21] also analyzed double-diffusive convection-radiation interaction on unsteady MHD flow over a vertical moving porous plate with heat generation and Soret effects, A. Bahloul *et al.* [22] studied double-diffusive and Soret induced convection in a shallow horizontal porous layer. Z. Alloui *et al.* [23] double-diffusive and Soret induced convection of a micropolar fluid in a vertical channel. N. Nithyadevi *et al.* [24] have studied double-diffusive natural convection in a partially heated enclosure with Soret and Dufour effects, Ziya Uddin *et al.* [25] have studied MHD heat and mass transfer free convection flow near the lower stagnation point of an isothermal cylinder imbedded in porous domain with the presence of radiation, A. Pantokratoras [26] has studied the effect of viscous dissipation in natural convection along a heated vertical plate, A. K. H. Kabir *et al.* [27] discovered the effects of viscous dissipation on MHD natural convection flow along a vertical wavy surface with heat generation. Osama Abu-Zeid [28] studied viscous and Joule heating effects over an isothermal cone in saturated porous media. Fully developed natural convection heat and mass transfer of a micropolar fluid in a vertical channel with asymmetric wall temperatures and concentrations was studied by C.Y. Cheng [29]. B. S. Malga *et al.* [30] have studied the finite element analysis for unsteady MHD heat and mass transfer free convection flow of polar fluids past a vertical moving porous plate in a porous medium with heat generation and thermal diffusion. Effect of viscous dissipation in natural convection was studied by Gebhart [31]. The present paper is the extension work of Z. Alloui *et al.* [23] by considering MHD free convection also convection induced by the viscous dissipation effects on fully developed natural convection of heat and mass transfer of a micropolar fluid in a vertical channel.

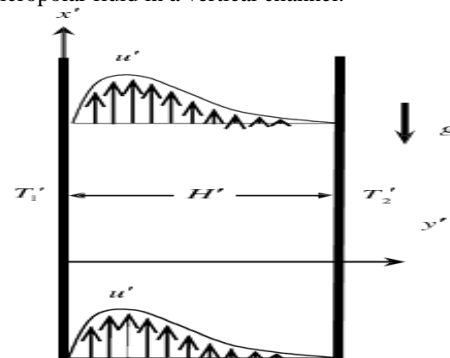


Figure (a). The flow configuration and the coordinate system.

2. Mathematical Model

We consider a steady fully developed laminar natural convection flow of a micropolar fluid between two infinite vertical plates (see Fig. (a)). The vertical plates are separated by a distance H' . The convection current is induced by both the temperature and concentration gradients. The flow is assumed to be in the x' direction, which is taken to be vertically upward along the channel walls, while the y' -axis is normal to the plates. The fluid is assumed to satisfy the Boussinesq approximation, with constant properties except for the density variations in the buoyancy force term.

The density variation with temperature and concentration is described by the state equation

$$\rho = \rho_o [1 - \beta'_T (T' - T'_o) - \beta'_C (C - C_o)]$$

where ρ_o is the fluid mixture density at temperature

$T' = T'_o$ and mass fraction $C = C_o$, and β'_T and β'_C

are the thermal and the concentration expansion coefficients, respectively. In the present investigation the viscous dissipation effects studied and the Dufour effect is neglected since it is well known that the modification of the heat flow due to the concentration gradient is of importance in gases but negligible in liquids. Equations (1)-(4) are Z. Alloui *et al.* [23] under these assumptions, the governing equations can be written as:

$$(\mu + \kappa) \frac{d^2 u'}{dy'^2} + \kappa \frac{dN'}{dy'} =$$

$$-\rho_o g [\beta'_T (T' - T'_o) - \beta'_C (C - C_o)] + \sigma B_o^2 u'$$

$$\frac{\gamma}{j} \frac{d^2 N'}{dy'^2} - \frac{\kappa}{j} \left(2N' + \frac{du'}{dy'} \right) = 0$$

$$\frac{d^2 T'}{dy'^2} + \frac{\nu}{\rho_o c_p} \left(\frac{du'}{dy'} \right)^2 = 0$$

$$\frac{d^2 C'}{dy'^2} = 0$$

where u' is the velocity component along the x' direction, and g is the acceleration due to gravity. Further, μ, κ, j, N' and γ are respectively the dynamic viscosity, vortex viscosity, micro-inertia density, angular velocity and spin gradient viscosity. Following Chamkha *et al.* [7] it is assumed that γ has the form

$$\gamma = (\mu + \kappa/2) j C_p$$

is the specific heat at constant pressure, ν is the kinematic viscosity $\nu = \frac{\mu}{\rho_o}$

The appropriate boundary conditions, applied on the walls of the vertical channel, are:

$$u' = 0, N' = -n \frac{du'}{dy'}, T' = T'_1, (1-a)C + a \frac{dC}{dy'} =$$

$$(1-a)C_1 - a \frac{D'}{D} C_o (1-C_o) \frac{dT'}{dy'} \quad \text{on } y' = 0 \quad (5)$$

$$u' = 0, N' = -n \frac{du'}{dy'}, T' = T'_2, (1-a)C + a \frac{dC}{dy'} =$$

$$(1-a)C_2 - a \frac{D'}{D} C_o (1-C_o) \frac{dT'}{dy'} \quad \text{on } y' = H' \quad (6)$$

where $0 \leq n \leq 1$ is a boundary parameter that indicates the degree to which the microelements are free to rotate near the channel walls. The case $n = 0$ represents concentrated particle flows in which the microelements close to the wall are unable to rotate S.K. Jena *et al.* [32]. Finally, according to Peddieson [33] the case $n = 1$ is applicable to the modeling of turbulent boundary layer flows. D and D' are respectively the molecular diffusion coefficient and the thermodiffusion coefficient.

The governing equations are non-dimensionalized by scaling length by H'

$$u' = \frac{\mu G_r}{\rho_o H' u}$$

$$N' = \frac{\mu G_r}{\rho_o H'^2 N}$$

$$G_r = g \rho_o^2 \beta'_T \frac{(T_1 - T_o) H'^3}{\mu^2}$$

$$M = \frac{\sigma B_o^2 H'^2}{\mu}$$

$$T = \frac{T' - T'_o}{T'_1 - T'_o}$$

$$S = \frac{C - C_o}{\Delta C}$$

$$\Delta T' = T'_1 - T'_o \quad \text{and}$$

$$\Delta C = C_1 - C_o \quad \text{for double - diffusive convection,}$$

$$\Delta C = -C_o (1 - C_o) \Delta T' \frac{D'}{D} \quad \text{for Soret - driven convection,}$$

$$E_c = \frac{\mu G_r}{(\rho_o H') \Delta t}$$

$$\varphi = \frac{\beta'_C \Delta C}{\beta'_T \Delta T'}$$

$$R_r = \frac{T'_2 - T'_o}{T'_1 - T'_o}$$

$$R_s = \frac{C_2 - C_o}{C_1 - C_o}$$

$$K = \frac{\kappa}{\mu}$$

$$B = \frac{H'^2}{j}$$

the subscript ' indicates a reference state.

The dimensionless equations governing the present problem then read

$$(1 + K) \frac{d^2 u}{dy^2} + K \frac{dN}{dy} = -[T + \varphi S] + Mu \tag{7}$$

$$\left(1 + \frac{K}{2}\right) \frac{d^2 N}{dy^2} - BK \left(2N + \frac{du}{dy}\right) = 0 \tag{8}$$

$$\frac{d^2 T}{dy^2} + E_c \left(\frac{du}{dy}\right)^2 = 0 \tag{9}$$

$$\frac{d^2 S}{dy^2} = 0 \tag{10}$$

The corresponding boundary conditions in dimensionless form are

$$u = 0, N = -n \frac{du}{dy}, T = 1, \tag{11}$$

$$(1 - a)S + a \frac{dS}{dy} = (1 - a) + a \frac{dT}{dy} \text{ on } y = 0$$

$$u = 0, N = -n \frac{du}{dy}, T = R_T, \tag{12}$$

$$(1 - a)S + a \frac{dS}{dy} = (1 - a)R_S + a \frac{dT}{dy} \text{ on } y = 1$$

In the present formulation the particular case $a = 0$ corresponds to double-diffusive convection for which the solutal buoyancy forces are induced by the imposition of a constant concentration such that $S = 1$ on $y = 0$ and $S = R_S$ on $y = 1$. On the other hand, $a = 1$ corresponds to the case of a binary fluid subject to the Soret effect. For this situation, it follows from Eqs. (11) and (12) that $dS/dy = dT/dy$ on $y = 0, 1$.

3. Method of Solution

It can be shown that Eqs. (7) - (10), together with the boundary conditions Eqs. (11) - (12) possess the following finite element solution, obtained with the help of the MATLAB software. In order to reduce the above system of differential equations to a system of dimensionless form, we may represent the velocity and microrotation, temperature and concentration by applying the Galerkin finite element method for equation (7) over a typical two-noded linear element (e), ($y_j \leq y \leq y_k$) is:

$$u = N \cdot \phi, \quad N = [N_j, N_k], \quad \phi = \begin{bmatrix} u_j \\ u_k \end{bmatrix},$$

$$N_j = \frac{y_k - y}{l}, \quad N_k = \frac{y - y_j}{l}, \quad l = y_k - y_j = h$$

$$\int_{y_j}^{y_k} N^T \left[(1 + K) \frac{d^2 u}{dy^2} + K \frac{dN}{dy} \right] dy = 0 \tag{13}$$

$$\int_{y_j}^{y_k} N^T \left[(1 + K) \frac{d^2 u}{dy^2} + Mu - R \right] dy = 0$$

where $R = K \frac{dN}{dy} + (T + \varphi S)$

The element equation given by

$$\int_{y_j}^{y_k} (1 + K) \begin{bmatrix} N'_j N'_j & N'_j N'_k \\ N'_k N'_j & N'_k N'_k \end{bmatrix} \begin{bmatrix} u_j \\ u_k \end{bmatrix} dy + M \begin{bmatrix} N_j N_j & N_j N_k \\ N_k N_j & N_k N_k \end{bmatrix} \begin{bmatrix} u_j \\ u_k \end{bmatrix} dy - R \begin{bmatrix} N_j \\ N_k \end{bmatrix} dy = 0 \tag{14}$$

where $S_M = \int_{y_j}^{y_k} (1 + K) \begin{bmatrix} N'_j N'_j & N'_j N'_k \\ N'_k N'_j & N'_k N'_k \end{bmatrix} \begin{bmatrix} u_j \\ u_k \end{bmatrix} dy + M \begin{bmatrix} N_j N_j & N_j N_k \\ N_k N_j & N_k N_k \end{bmatrix} \begin{bmatrix} u_j \\ u_k \end{bmatrix} dy$ and $R^* = R \begin{bmatrix} N_j \\ N_k \end{bmatrix} dy$

$$S_M = \frac{(1 + K)}{l} \begin{bmatrix} 1 & -1 \\ -1 & 1 \end{bmatrix} \begin{bmatrix} u_j \\ u_k \end{bmatrix} + \frac{Ml}{6} \begin{bmatrix} 1 & 2 \\ 2 & 1 \end{bmatrix} \begin{bmatrix} u_j \\ u_k \end{bmatrix}$$

and $R^* = R \frac{l}{2} \begin{bmatrix} 1 \\ 1 \end{bmatrix}$

We write the element equation for the elements ($y_{i-1} \leq y \leq y_i$) and ($y_i \leq y \leq y_{i+1}$). Assembling these element equations, we get

$$\frac{(1 + K)}{l} \begin{bmatrix} 1 & -1 & 0 \\ -1 & 2 & -1 \\ 0 & -1 & 1 \end{bmatrix} \begin{bmatrix} u_{i-1} \\ u_i \\ u_{i+1} \end{bmatrix} + \tag{15}$$

$$\frac{Ml}{6} \begin{bmatrix} 2 & 1 & 0 \\ 1 & 4 & 1 \\ 0 & 1 & 2 \end{bmatrix} \begin{bmatrix} u_{i-1} \\ u_i \\ u_{i+1} \end{bmatrix} = R \frac{l}{2} \begin{bmatrix} 1 \\ 2 \\ 1 \end{bmatrix}$$

Now put row corresponding to the node i to zero, from equation (15) the difference schemes with $l=h$ is

$$\frac{(1 + K)}{h} (-u_{i-1} + 2u_i - u_{i+1}) + \tag{16}$$

$$\frac{Mh}{6} (u_{i-1} + 4u_i + u_{i+1}) = R^*$$

Using the Crank-Nicolson method to the equation (16), we obtain:

$$A_1 u_{i-1}^{j+1} + A_2 u_i^{j+1} + A_3 u_{i+1}^{j+1} = A_4 u_{i-1}^j + A_5 u_i^j + A_6 u_{i+1}^j + R^* \tag{17}$$

Similarly, the equations (8), (9) and (10) are becoming as follows:

$$B_1 N_{i-1}^{j+1} + B_2 N_i^{j+1} + B_3 N_{i+1}^{j+1} =$$

$$B_4 N_{i-1}^j + B_5 N_i^j + B_6 N_{i+1}^j + R_1^* \quad (18)$$

$$C_1 T_{i-1}^{j+1} + C_2 T_i^{j+1} + C_3 T_{i+1}^{j+1} =$$

$$C_4 T_{i-1}^j + C_5 T_i^j + C_6 T_{i+1}^j + R_2^* \quad (19)$$

$$D_1 S_{i-1}^{j+1} + D_2 S_i^{j+1} + D_3 S_{i+1}^{j+1} =$$

$$D_4 S_{i-1}^j + D_5 S_i^j + D_6 S_{i+1}^j \quad (20)$$

$$A_1 = \left(\frac{Mh}{6} - \left(\frac{1+k}{h} \right) \right), \quad A_2 = \left(\frac{Mh}{3} + 2 \left(\frac{1+k}{h} \right) \right),$$

$$A_3 = \left(\frac{Mh}{6} - \frac{1+k}{h} \right), \quad A_4 = \left(\left(\frac{1+k}{h} \right) - \frac{Mh}{3} \right),$$

$$A_5 = - \left(\frac{Mh}{3} + 2 \left(\frac{1+k}{h} \right) \right), \quad A_6 = \left(\left(\frac{1+k}{h} \right) - \frac{Mh}{6} \right)$$

$$B_1 = \left(\frac{hBK}{3} - \left(\frac{1+\frac{k}{2}}{h} \right) \right), \quad B_2 = \left(\frac{4hBk}{3} + 2 \left(\frac{1+\frac{k}{2}}{h} \right) \right),$$

$$B_3 = \left(\frac{hBK}{3} - \frac{1+\frac{k}{2}}{h} \right), \quad B_4 = \left(\left(\frac{1+\frac{k}{2}}{h} \right) - \frac{hBK}{3} \right),$$

$$B_5 = - \left(\frac{4hBK}{3} + 2 \left(\frac{1+\frac{k}{2}}{h} \right) \right), \quad B_6 = \left(\left(\frac{1+\frac{k}{2}}{h} \right) - \frac{BK h}{3} \right)$$

$$C_1 = -\frac{1}{h}, \quad C_2 = \frac{2}{h}, \quad C_3 = -\frac{1}{h}, \quad C_4 = \frac{1}{h}, \quad C_5 = -\frac{2}{h}, \quad C_6 = \frac{1}{h}$$

$$D_1 = -\frac{1}{h}, \quad D_2 = \frac{2}{h}, \quad D_3 = -\frac{1}{h}, \quad D_4 = \frac{1}{h}, \quad D_5 = -\frac{2}{h}, \quad D_6 = \frac{1}{h}$$

$$R^* = h \left(K \left(\frac{N_{i+1} - N_{i-1}}{h} \right) + T + \varphi S \right),$$

$$R_1^* = -hK \left(\frac{u_{i+1} - u_{i-1}}{h} \right), \quad R_2^* = -hE_c \left(\frac{u_{i+1} - u_{i-1}}{h} \right)^2$$

Here $r = k / h^2$ where k, h is mesh sizes along y direction and x direction respectively. Index i refers to space and j refers to time. The mesh system consists of $h=0.1$ for velocity profiles and concentration profiles and $k=0.1$ has been considered for computations. In equations (8)-(10), taking $i=1(1) n$ and using initial and boundary conditions (11) and (12), the following system of equation are obtained:

$$A_i X_i = B_i, \quad i = 1, 2, 3, \dots \quad (21)$$

Where A_i 's are matrices of order n and X_i and B_i 's are column matrices having n -components. The solution of above system of equations are obtained using Thomas algorithm for velocity, angular velocity and temperature. Also, numerical solutions for these equations are obtained by MATLAB program. In order to prove the convergence and stability of Galerkin finite element method, the same MATLAB-Program was run with slightly changed values

of h and k , no significant change was observed in the values of μ, N, T, S

4. Results and Discussion

The numerical computations for the velocity u , angular velocity fields N for various governing parameters the buoyancy ratio φ , vortex viscosity parameter K , dimensionless microgyration n and constant a are illustrated in the graphs. Figure 1 illustrates the influence of vortex viscosity parameter K on the distribution of velocity u and microrotation N for $n=0, a=0$ and for $\varphi=5$ in Fig.1(a) and $\varphi=-5$ in Figure1(b). It is observed that with the increasing the value of K the intensity of convective velocity u is reduced as compared to the Newtonian fluid situation ($K=0$). In fact, it is found that as $K \rightarrow \infty, u \rightarrow 0$. The influence of parameter K on the microrotation N it is noticed that the variation with K of the value of N evaluated at the position half of the channel also presented in the graphs it can be seen that the intensity of N first increases with increase of K , the reverse phenomenon is observed later.

Figure 1(b) shows the results obtained from $\varphi=-5$, i.e., when thermal and solutal buoyancy forces are opposing each other for this situation in case of double-diffusive convection indicates that the flow direction is downwards, since the solutal buoyancy forces predominant. The velocity profiles increases with the increase of K are observed from Figure 1(b). It is seen that for $K=0$ when $N=0$, since no rotation can be occur in the absence of micropolar elements (Newtonian fluid situation). Microrotation N decreases with the increase of K up to half of the channel whereas microrotation N flow direction is now downward and the reverse phenomenon is observed.

The effect of buoyancy ratio φ velocity u , microrotation N exemplified in Figure 2 for the case $a=0, n=0, K=5$ in the absence of solute concentration effect i.e. when $\varphi=0$ the flow is induced solely by the imposed temperature gradients. It is observed from this figure when $\varphi < 0$ the thermal and solutal buoyancy forces act in the same direction and the flow is considered to aided thus the magnitude of the fluid of the fluid velocity and microrotation promoted in the vertical channel on the other hand when $\varphi < 0$ the solutal and buoyancy forces acts in opposite direction as a result the flow direction is now reversed since it is governed by the predominant solutal effects.

Figure 3 depicts the influence of micropolar parameter n velocity u , microrotation N profiles $K=5, \varphi=10$ and $a=0$, it can be seen from this figure, upon increase the value of n , the concentration of the solution becomes weaker such that the particles near the walls are free to rotate, which results in an enhancement of the flow. It is also seen that the velocity u increases with the increase of n .

The effect of magnetic field parameter M on the velocity profiles u and microrotation N for $K=5, \varphi=5$ when $a=0$ is shown in Figure 4 (a) and $K=5, \varphi=-5$ when $a=0$ is shown in Figure 4 (b). Here it is observed that the velocity profiles decrease with an increase of M , microrotation profiles increase up to the center of the channel, the reverse phenomenon is observed in the other part of the channel. Figure 4 (b) indicates that the velocity flow

direction is now downward for $\phi=-5$, since the solute buoyancy forces are free dominant. It can be seen that the velocity profiles u increase with an increase of M . The microrotation N decreases with the increase of M , up to

the middle of the channel (flow direction is upward) and it increases with the increase of M , observed in the other part of the channel.

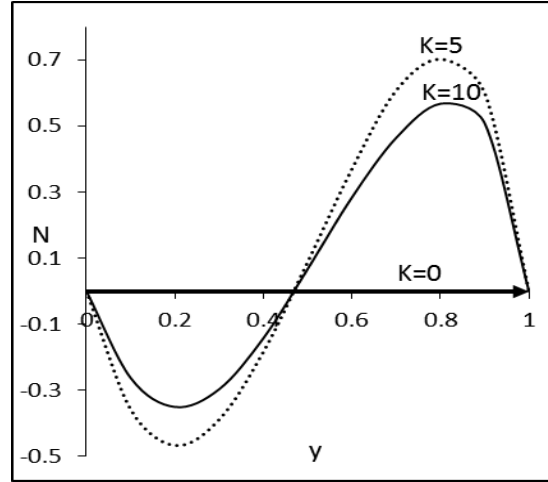
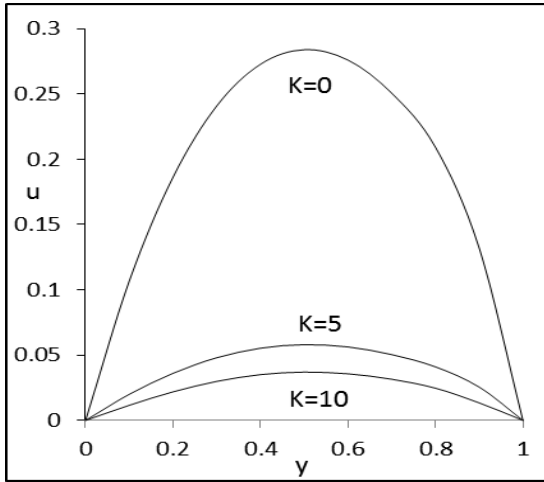


Figure 1(a). Effect of Parameter K on the velocity profiles u and the microrotation N for $n=0$, $a=0$ and $\phi=5$.

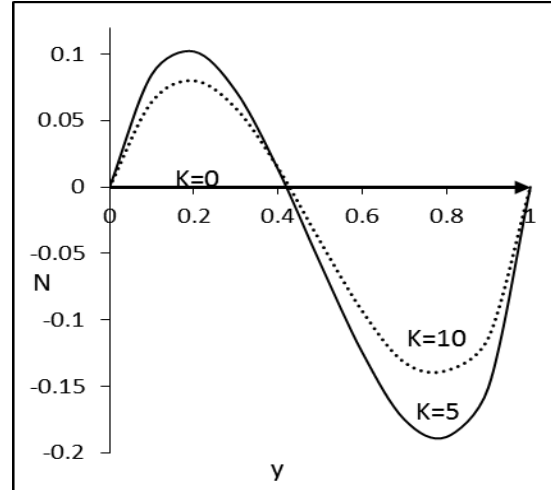
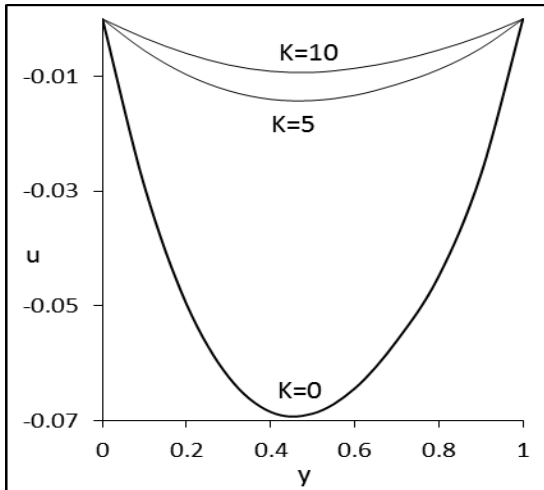


Figure 1(b). Effect of Parameter K on the velocity profiles u and the microrotation N for $n=0$, $a=0$ and $\phi=5$.

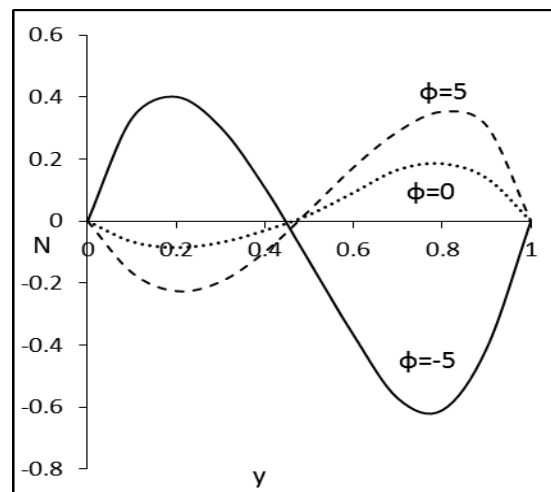
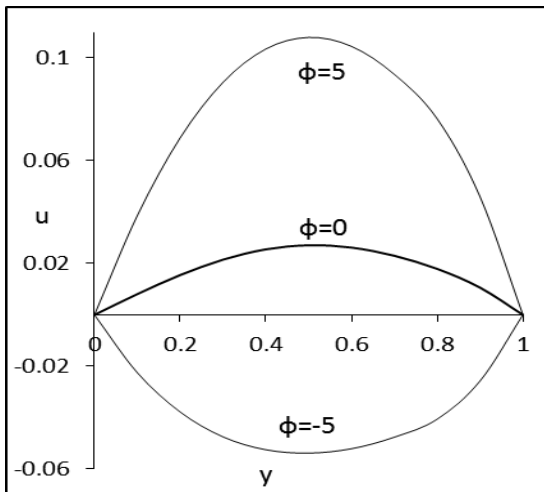


Figure 2. Effects of buoyancy ratio ϕ on the velocity profiles u and the microrotation profiles N for $K=5$, $n=0$ and $a=0$.

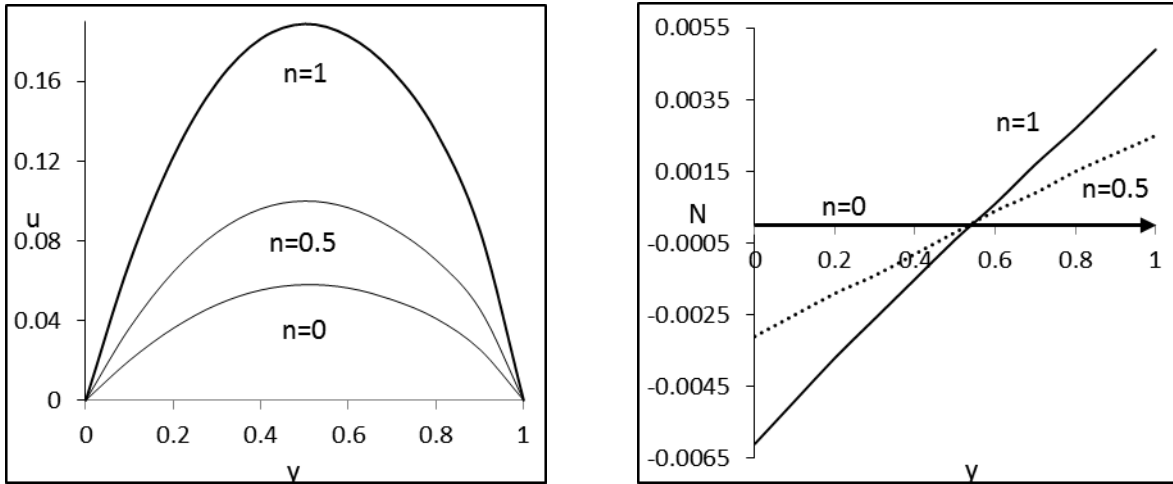


Figure 3. Effects of parameter n on the velocity profiles u and the microrotation profiles N for $K = 5, \varphi = 10$ and $a = 0$.

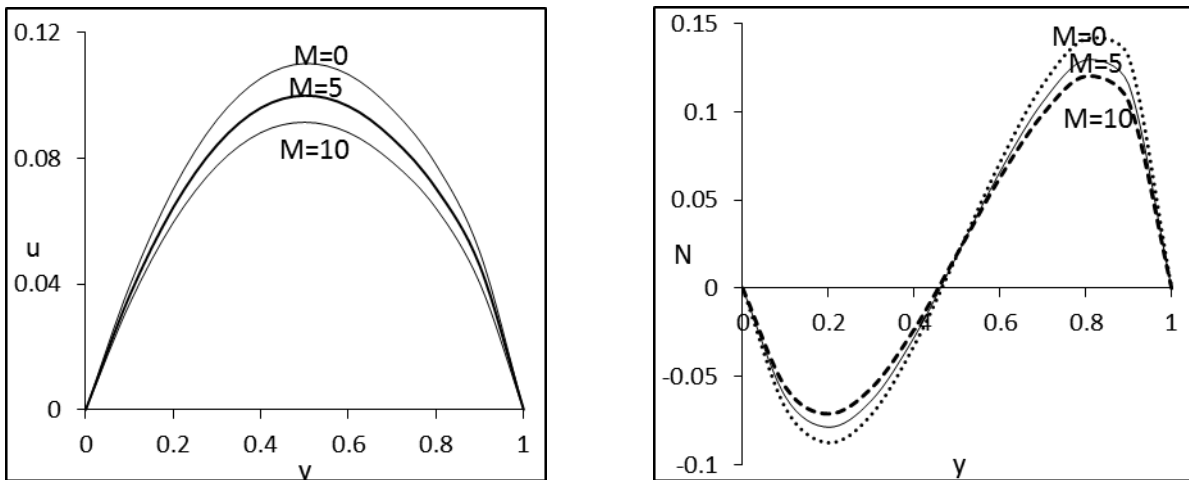


Figure 4(a). Effects of parameter M on the velocity profiles u and the microrotation profiles N for $K = 5, \varphi = 5$ and $a = 0$.

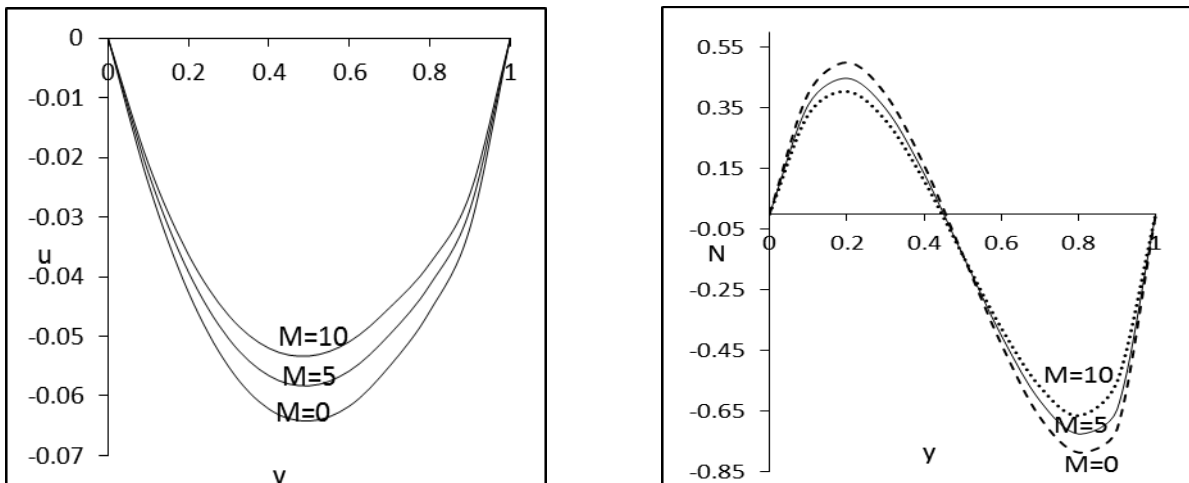


Figure 4(b). Effects of parameter M on the velocity profiles u and the microrotation profiles N for $K = 5, \varphi = -5$ and $a = 0$.

Figures 5-10 show that the velocity profiles u and microrotation N for different values of flow parameter when $a=1$. The effect of magnetic parameter M on the velocity profiles u and microrotation N for $K=5, \varphi=5$ is shown in Figure 5 (a) and $K=5, \varphi=-5$ is shown in Figure 5 (b), it remains the same when compared with $a=0$ in the present case $a=1$. The effect of vortex viscosity parameter K , on the velocity profiles u and microrotation N are shown in Figure 6 for both $\varphi=5$ and $\varphi=-5$ in the case of $a=1, n=0$, the effect of K is the same in both cases $a=0$

and $a=1$, whereas in the present case ($a=1$) for $\varphi=-5$ from Figure 6 (b) it indicates that the flow direction is upward in the present case, whereas it is downward in case $a=0$. It is also noticed that the effect of K decreases the velocity profiles u , the microrotation N decreases up to half of the channel and decreases the other part of the channel, as observed with the effect of K ; the reverse phenomenon is also observed in the present case ($a=1$) when compared to $a=0$.

The buoyancy ratio parameter ϕ effect on the velocity profiles u and microrotation N are shown in Figure 7. It is clear that the velocity profiles u increase with the increase of ϕ from 0 to 10, whereas they decrease from 0 to -10. However, upon increasing ϕ , considerably the flow pattern depends on the sign of the parameter up or down in the halves of the channel. It can also be seen that the microrotation profiles N decrease with the increase of ϕ from 0 to 10 and increase with the decrease of ϕ from 0 to -10, in the first half of the channel, as indicated from the Figure7, and the reverse phenomenon is observed in the other half of the channel.

Figure 8 illustrates the influence of micro-gyration parameter n on velocity u and microrotation N for $\phi=10$, $K=5$, $a=1$. It is noticed that the velocity u increases with the increase of n . In the present case for $a=1$, the results indicate the intensity of convective flow u and that of the angular velocity N are minimum for $n = 0$. This particular value of n represents the case where the concentration of the microelements is sufficiently large that the particles close to the walls are unable to rotate. Upon increasing the value of n , the concentration of the solution becomes weaker such that the particles near the walls are free to rotate. Thus, as n is augmented the microrotation term is augmented, which induces an enhancement of the flow.

Figures 9 (a) & (b) illustrate the volume flow rate Q with the buoyancy ration parameter ϕ , when $K=1.5$, for the various values of micro-gyration parameter n at $a=0$ and $a=1$ for the case of double-diffusive convection it is observed that when both the thermal and solutal buoyancy

forces are aiding ($\phi > 0$), the flow direction is upward ($Q > 0$). The reverse is true ($Q < 0$) when both the thermal and solutal buoyancy forces are opposing ($\phi < 0$). On the other hand, for the case of soret induced convection, the flow rate is found to be independent of the buoyancy ratio ϕ . This follows the fact that, for this situation, the quantity of the solute between the two vertical plates remains constant. The Soret effect acts merely to redistribute the concentration in the system, giving rise to local increase or decrease of the local velocity. However, the global flow rate remains constant. Also, as discussed above, upon increasing the value of n the intensity of the velocity field (and thus of the flow rate Q) is enhanced.

The dimensionless total rate, E , at which heat is added to the fluid, is plotted in Figure 10 (a) and (b) as a function of the buoyancy ratio ϕ and the micro-gyration parameter n , for the case $K = 1.5$. Figure 10 (a) shows that, in the case of double diffusive convection, for ($\phi > 0$), increasing ϕ results in an augmentation of the strength of the convective motion such that E increases. For ($\phi < 0$), the results are similar but, since the flow direction is now downward, the value of E is negative. On the other hand, the results obtained for soret-induced convection, Figure 10 (b), are quite different. For this situation, the velocity profiles (not presented here) indicate that for ($\phi \gg 0$) the flow is upward near the left hotter wall and downward near the right colder one. Thus, the total rate E , at which heat is added to the fluid, is promoted upon increasing ϕ as a result of the increase of the flow intensity near the hotter wall.

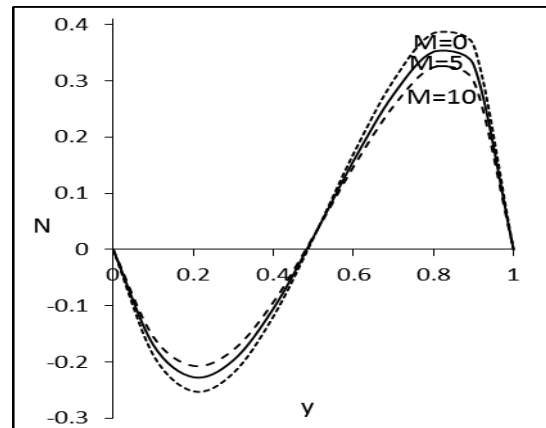
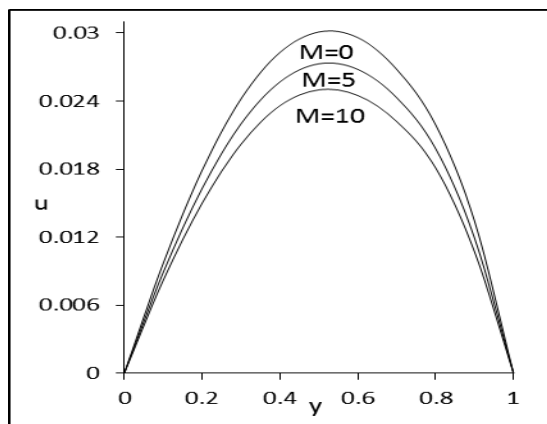


Figure 5(b). Effects of parameter M on the velocity profiles u and the microrotation profiles N for $K = 5$, $\phi = -5$ and $a = 1$.

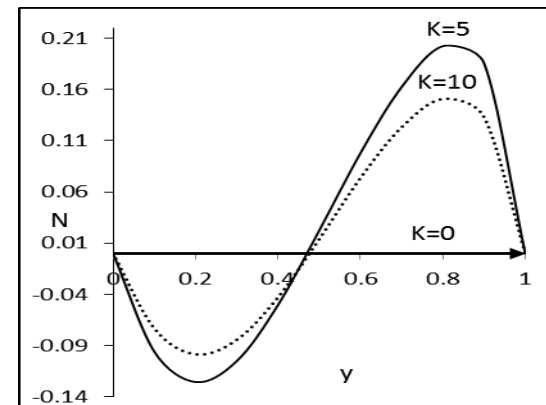
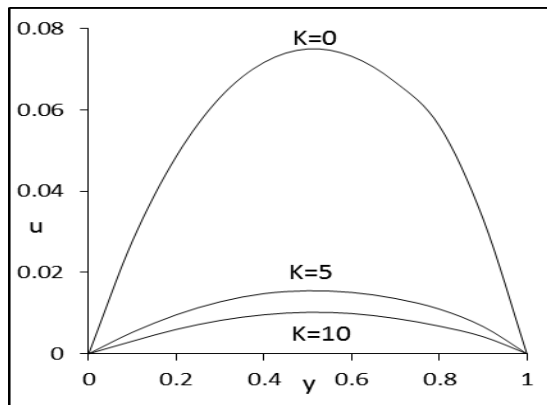


Figure 6(a): Effect of Parameter K on the velocity profiles u and the microrotation N for $n=0$, $a=1$ and $\phi=5$.

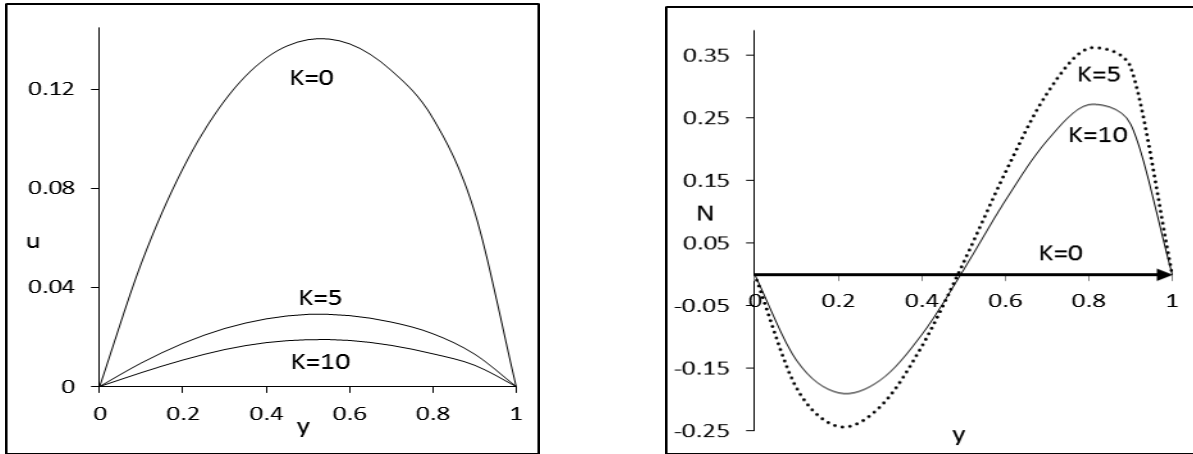


Figure 6(b): Effect of Parameter K on the velocity profiles u and the microrotation N for $n=0$, $a=1$ and $\phi=5$.

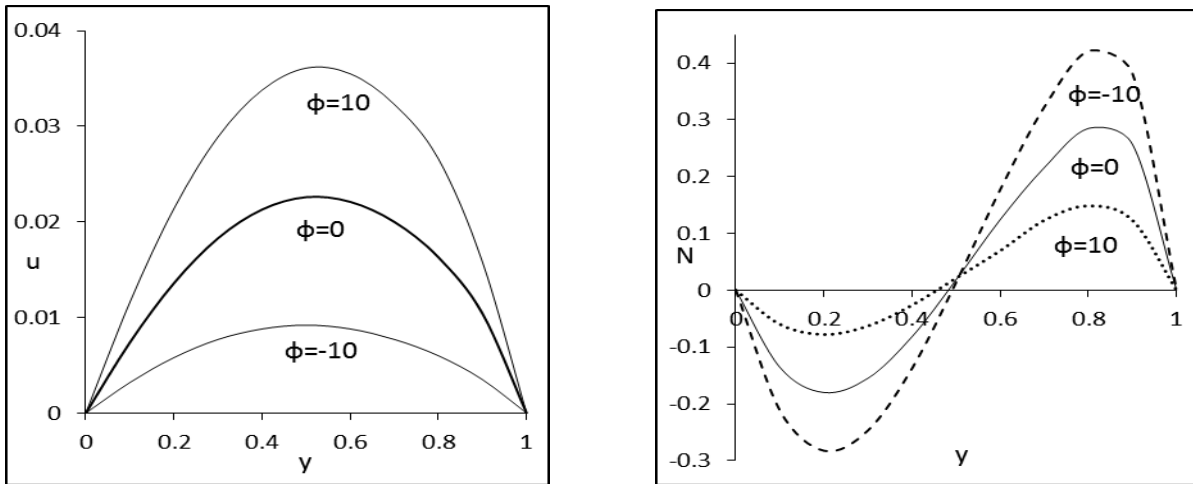


Figure 7. Effects of buoyancy ratio ϕ on the velocity profiles u and the microrotation profiles N for $K=5$, $n=0$ and $a=1$.

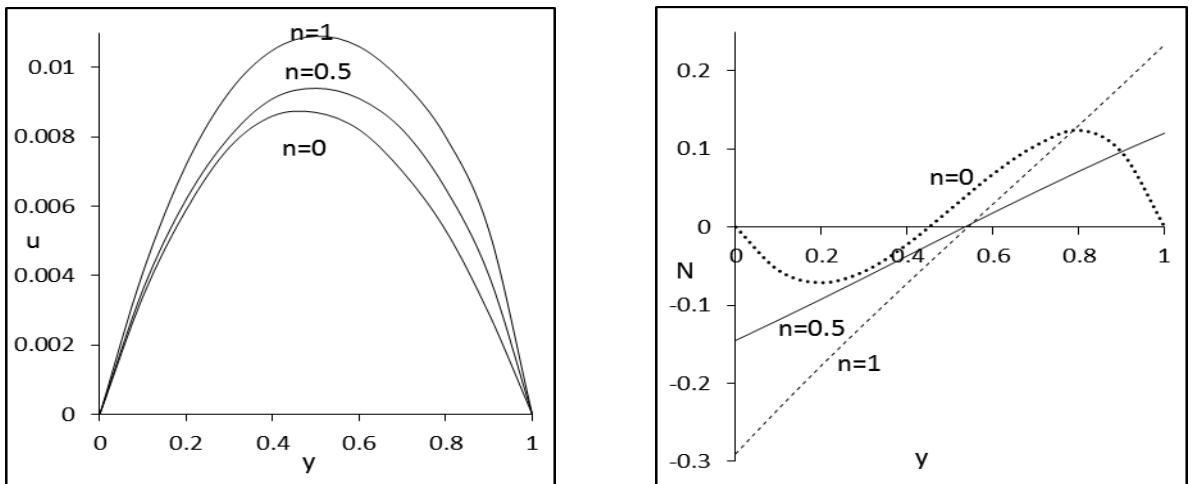


Figure 8. Effects of parameter n on the velocity profiles u and the microrotation profiles N for $K=5$, $\phi=10$ and $a=1$.

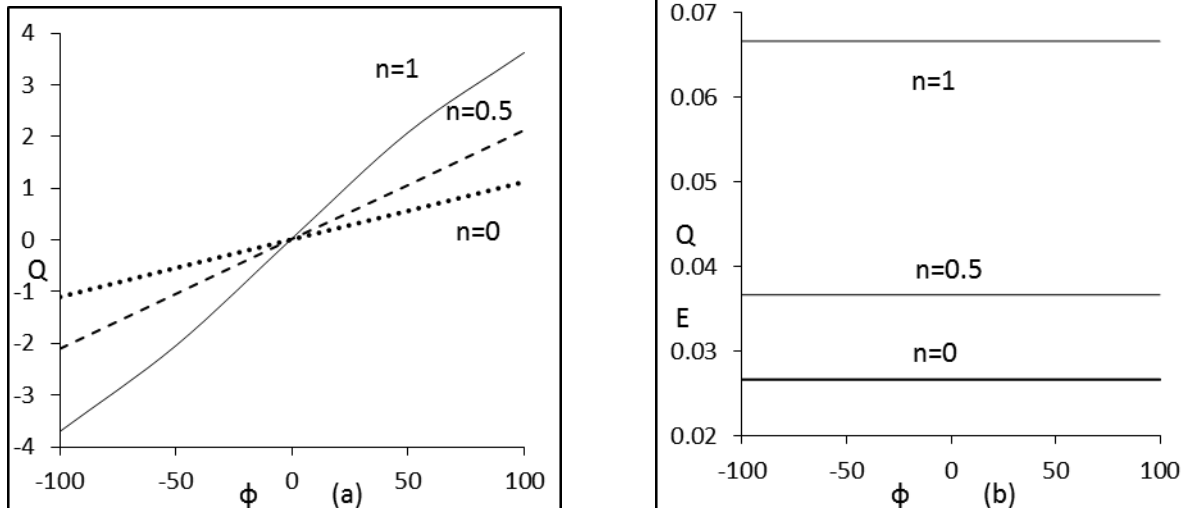


Figure 9. Effects of buoyancy ratio ϕ and parameter n on the volume flow rate Q for $K = 1.5$, (a) $a = 0$, (b) $a = 1$.

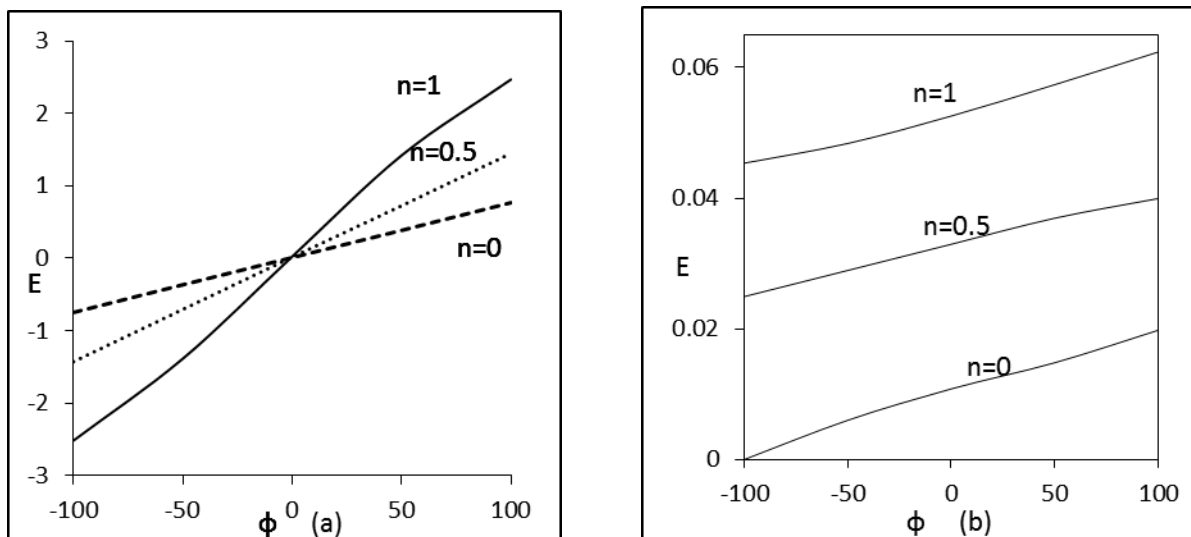


Figure 10. Effects of buoyancy ratio ϕ and parameter n on the total rate at which heat is added to the fluid, E , for $K = 1.5$, $a = 0$, (b) $a = 1$.

Let's now consider the buoyancy ratio. The dimensionless total rate, Φ , at which species are added to the fluid, is depicted in Figure 11 as a function of ϕ and the micro-gratation parameter n , for the case $K = 1.5$. The Soret-induced convection, represented by a dotted line, indicates that $\Phi = 0$ independently of n . This is expected since, for this situation, the solid boundaries are impermeable to concentration. The Soret effect is merely to redistribute the originally uniform concentration within the system. However, for double diffusion, the solid lines indicate that increasing ϕ , i.e., increasing the strength of the convective flow, results in an enhancement of the rate of mass transfer through the system. These results are similar to those reported by Z. Alloui *et al.* [23]. Also, it is observed from Figure 11 that, for a given value of ϕ , Φ decreases as the value of n is reduced toward $n = 0$. As already mentioned, a decrease of n corresponds to an increase of the concentration of the solution such that the particles close to the solid boundaries are unable to rotate. This results in a decrease of the flow rate and thus a decrease of Φ . The volume flow rate, Q , and total rate at which heat is added to the fluid, E , are plotted in Figure 12 as a function of K for $\phi = 2$ and $n = 0$. Here again, the results obtained for double-diffusive convection and Soret-

induced convection are qualitatively similar. In the limit $K \rightarrow 0$ both Q and E tend asymptotically to constant values corresponding to the Newtonian fluid situation. On the other hand, in the limit $K \rightarrow \infty$, both Q and E become negligible, due to the increase of the vortex viscosity.

It is seen from the Figure 13 for the values of magnetic parameter $M = 0, 5, 10$, the velocity decreases up to the position of $y=0$. At the position of $y=5$, velocity becomes constant, that is, velocity profiles meet at a point and then cross the side and increasing with magnetic parameter M . This is because of the velocity profiles, with lower peak values for higher values of magnetic parameter M , tend to decrease comparatively slower along y -direction than velocity profiles with higher peak values for lower values of magnetic parameter M . We may conclude that for increasing values in M ; the Lorentz force, which opposes the flow, there is a fall in velocity maximum due to the retarding effect of the magnetic force in the region. As a result, the momentum boundary layer thickness becomes larger and the separation of the boundary layer will occur earlier. Here, it is observed that the increase in the viscous dissipation (Ec) decreases the velocity.

It is also observed from Figure 14 that as the viscous dissipation parameter (Ec) increases, the temperature profiles increase. The increase in the viscous dissipation cools the fluid. The temperature profile for various values of the viscous dissipation parameter (Ec) while the other parameters are kept constant. It is found that the increase in viscous dissipation parameter (Ec) leads to a corresponding increase in the temperature profile. It is also seen that the temperature decreases at a certain portion of the channel and then increases, this could be due to the dissipation effect and the harmonic pressure term.

It is known that the viscous dissipation produces heat due to a drag between the fluid particles and this extra heat causes an increase of the initial fluid temperature (see Figure 14). This increase of temperature causes an increase of the buoyant force. The increase of the buoyant force causes an increase of the fluid velocity. The bigger fluid velocities cause a bigger drag between the fluid particles and consequently bigger viscous heating of the fluid. The new increase of fluid temperature influences the buoyant force and this procedure goes on. There is a continuous interaction between the viscous heating and the buoyant

force. This mechanism produces different results in the upward and downward flow. In the upward flow, where the fluid is warmer than the ambient, the extra viscous heat is added to the initial heat (the warm fluid becomes warmer) and the fluid velocity increases. In the downward flow, the fluid is cooler than the ambient and the viscous heating causes an increase in the initial fluid temperature (the cold fluid becomes warmer).

In many material processing applications, such as extrusion hot rolling, drawing and continuing costing, materials continuously move a channel. In such industrial applications, it is of great importance to encounter the heat transfer from the moving boundary to the surrounding fluid and vice versa. However, the moving boundaries deform the fluid velocity profiles and shear the fluid layer near the boundary resulting in local changes in velocity gradient thus the Eckert number effects may not be neglected in heat transfer analysis, associated with moving boundaries. The thermal energy generated due to Eckert number is significant near the wall, which alters the heat transfer rates following the changes in the temperature profiles.

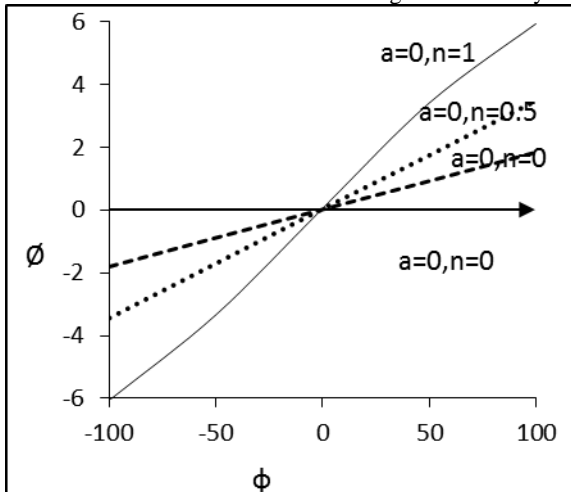


Figure 11. Effects of parameter K on the volume flow rate Q total rate at which heat is added to the fluid for $\phi = 2$ and $n = 0$.

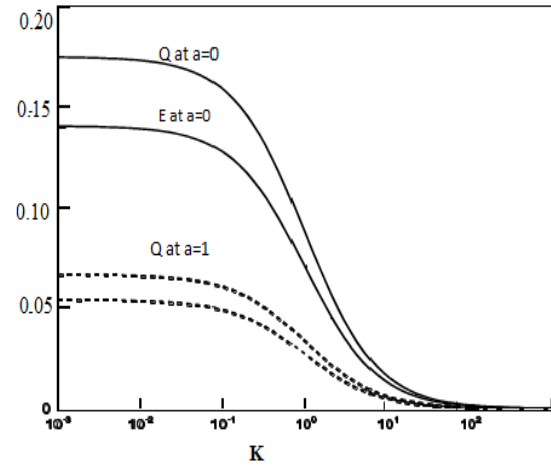


Figure 12. Effects of parameter K on the volume flow rate Q and on the total rate at which heat is added to the fluid for $\phi = 2$ and $n=0$

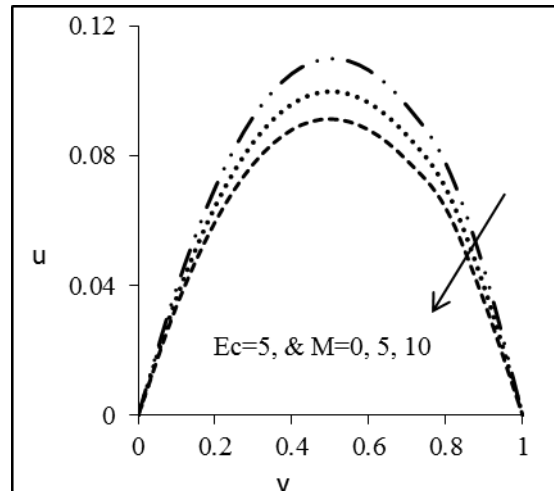
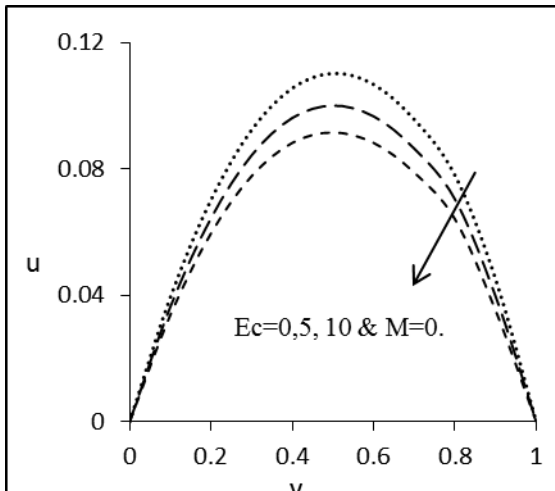


Figure 13. Effects of Viscous dissipation (Ec) on the Velocity Profiles u

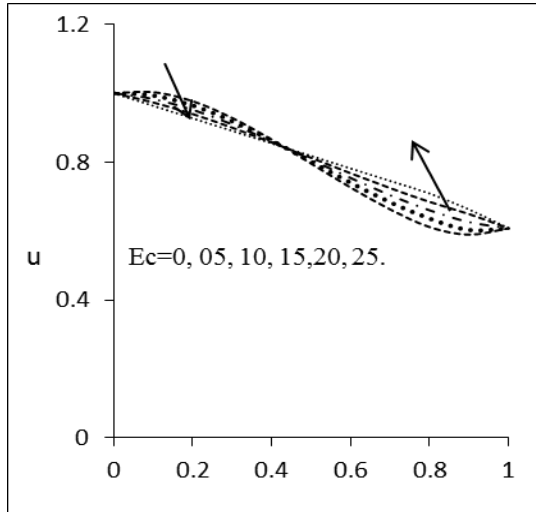


Figure 14. Effects of Viscous dissipation(Ec) on the Temperature Profiles T

Table. 1 presents a comparison between the numerical, analytical and present solution for $K=1.5, B = 1, \phi = 2, R_T = 0.6, R_S=0.3, n = 0$ and $a = 0$. It must be mentioned that in the case of $a = 0$ and $n = 0$ the present results are similar to those reported by Z. Alloui *et al.* [23]. There is a good agreement with the previous author's results.

Table 1. Presents a comparison between the numerical, analytical and present solution for $K = 1.5, B = 1, \phi = 2, R_T = 0.6, R_S = 0.3, n = 0$ and $a = 0$.

Profiles	Analytical	Numerical Analytical	Present
u	1.06092	1.06092	1.05925
N	0.14075	0.14075	0.14078

Skin Friction (Shear stress) and Nusselt number (Rate of Heat Transfer)

$$\text{Nusselt number (rate of heat transfer)} = \frac{H'}{\kappa(T_1 - T_o)} = \frac{dT}{dy} \Big|_{y=0}$$

$$\text{Skin friction (Shear stress)} = \frac{2\tau_w}{\rho_o u^2} = \frac{du}{dy} \Big|_{y=0}$$

The profiles for skin friction and the rate of heat transfer with viscous dissipation (Ec) parameter are shown graphically in Figure 15, depicting the distribution of the skin friction with the variation of material parameter, magnetic parameter and viscous dissipation parameter. It is clear from the figure that for assisting flow skin friction decreases with the increase of material parameter and magnetic parameter, while a reverse pattern is observed for opposing flow. The rate of heat transfer increases with an increase in viscous dissipation (Ec) parameter. Thus, fast cooling of the plate can be achieved by increasing a/c . It can also be obtained by increasing the material parameter, magnetic field parameter for the opposing flow while for assisting flow, fast cooling of the plate can also be achieved by decreasing the material parameter or magnetic parameter.

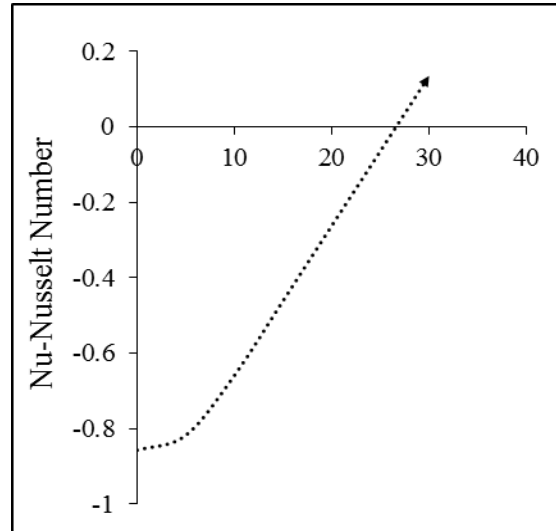


Fig. 15(a). Ec-Viscous dissipation

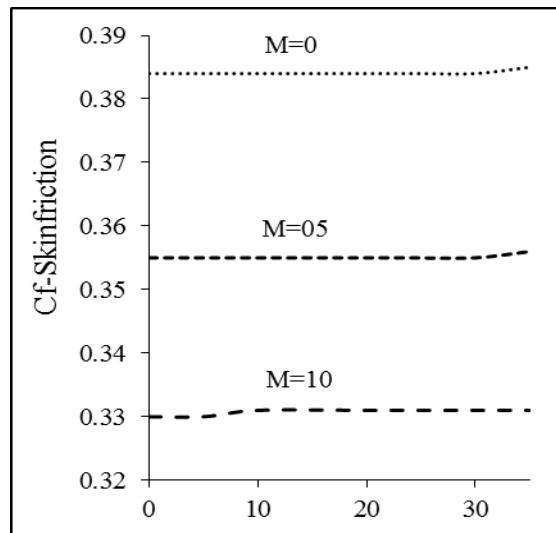


Fig. 15(b). Ec-Viscous dissipation

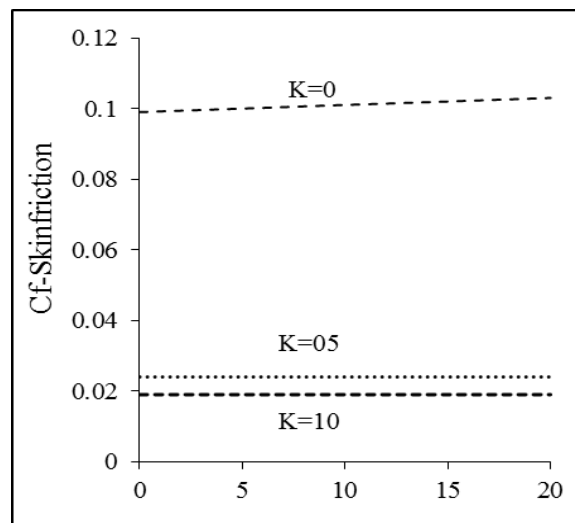


Fig. 15(c). Ec-Viscous dissipation

Conclusions

In this paper we have studied fully developed free convection flow heat and mass transfer of a MHD/micropolar fluid over a vertical channel. The cases of fully developed convection and viscous dissipation effect are investigated. Asymmetric wall temperatures and concentrations are considered.

- The closed form solution proposed in this paper, for fully developed flow, is found to be in excellent agreement with a numerical solution of the time dependent form of the governing equations. Thus, in the range of the governing parameters considered in this study, the solution is steady.
- In general, it is found that upon increasing the vortex viscosity parameter K , the fluid velocity is inhibited. The influence of micro-rotation parameter n , which characterizes the boundary conditions applied on rotation of the microelements near the solid boundaries, on the velocity u and microrotation N profiles is found to be significant. Thus, as n is augmented, the microrotation term is promoted, which induces enhancement of flow velocities.
- The effect of the buoyancy ratio ϕ on the velocity profiles u and microrotation profiles N is also found to be important. The flow direction in the channel depends strongly on the sign of this parameter. The results presented in this paper illustrate the difference between double diffusion [13] and Soret-induced convection.
- For instance, the rate of flow Q within the channel is found to be independent of the buoyancy ratio ϕ . This is not the case for double-diffusive convection where Q is observed to depend considerably upon ϕ . Also the results indicate that, for given values of ϕ and n , the influence of K on u and N is higher for $a = 0$ than $a = 1$. A similar trend is observed for the effect of ϕ on u and N , for fixed values of K and n .
- The total rate at which heat is added to the fluid is found to be considerably higher for double diffusion than Soret convection. Finally, it must be mentioned that in the case of $a = 0$ and $n = 0$ the present results are similar to those reported by Chen [34]. As regards the Soret-induced convection, this flow configuration does not seem, to the best of authors' knowledge, to have been investigated previously.
- For the values of magnetic parameter $M = 0, 5, 10$, the velocity decreasing up to the position of $y=0$. At the position of $y=4.5$ velocity becomes constant that is velocity profiles meet at a point and then cross the side and increasing with magnetic parameter M . It is also found that increase in viscous dissipation parameter (Ec) leads to a corresponding increase in the velocity. It is also seen that the velocity decreases at a certain portion of the channel and then increases; this could be due to the dissipation effect.
- It is found that the increase in viscous dissipation parameter (Ec) leads to a corresponding increase in the temperature profile. It is also seen that the temperature decreases at a certain portion of the channel and then increases; this could be due to the dissipation effect and the harmonic pressure term.
- The Eckert number (Ec) is the ratio of kinetic energy of the flow to the boundary layer enthalpy difference. The

effect of Eckert number (Ec) on flow field is to increase the energy, yielding a greater fluid temperature and as a consequence greater buoyancy forces, the increasing on the buoyancy forces due to an increase in the dissipation parameter hence the temperature.

References

- [1] A.C. Eringen, "Theory of micropolar fluids, Journal of Mathematics Mechanics", Vol.16, 1966, 1-18.
- [2] A.C. Eringen, "Nonlinear theory of simple micro-elastic solids", International Journal of Engineering Science, Vol.2, 1964, 189-203.
- [3] A.C. Eringen, "Theory of thermomicropolar fluids", Journal of Mathematical Analysis and Applications, Vol.38, 1972, 480-496.
- [4] I. Papautsky, J. Brazzle, T. Ameel, A.B. Frazier, "Laminar fluid behavior in microchannels using micropolar fluid theory", Sensors Actuators Vol.73, 1999, 101-108.
- [5] T. Ariman, M.A. Turk, N.D. Sylvester, "Applications to microcontinuum fluid mechanics a review", International Journal of Science, Vol.12, 1974, 273-293.
- [6] G. Lukaszewicz, Micropolar Fluids, "Theory and Applications", Birkhauser, Basel, 1999.
- [7] A.J. Chamkha, T. Grosan, I. Pop, "Fully developed free convection of a micropolar fluid in a vertical channel", International Communications of Heat Mass Transfer, Vol.29, 2002, 1119-1127.
- [8] J.P. Kumar, J.C. Umavathi, Ali J. Chamkha, I. Pop, "Fully-developed free convection of micropolar and viscous fluids in a vertical channel", Applied Mathematical Modelling, Vol.34, 2010, 1175-1186.
- [9] A.S. Bataineh, M.S.M. Noorani, I. Hashim, "Solutions of fully developed free convection of micropolar fluid in a vertical channel by homotopy analysis method", International Journal of Numerical Methods Fluids, Vol.60, 2009, 779-789.
- [10] O. Abdulaziz, I. Hashim, "Fully developed free convection heat mass transfer of a micropolar fluid between porous vertical plates", Numerical Heat Transfer Part A-applications, Vol.55, 2009, 270-288.
- [11] Nield, D. A., "The thermohaline Rayleigh-Jeffrey's problem", Journal of Fluid Mech, Vol. 29, 1967, 545- 558.
- [12] Taunton, J. W., Lightfoot, E. N. & Green. T., "Thermohaline instability and salt fingers in a porous medium", Phys. Fluids, Vol.15, 1972, 748-753.
- [13] Poulidakos. D., "Double diffusive convection in a horizontal sparcely packed porous layer", International omunications of Heat Mass Transfer, Vol.13, 1986, 587-598.
- [14] Brand. H. R, Steinberg. V., "Convective instabilities in binary mixtures in a porous medium", Physica A, Vol.119, 1983a, 327-338.
- [15] Brand. H. R., Steinberg. V., "Nonlinear effects in the convective instability of a binary mixture in a porous medium near threshold", Physics Letters A, Vol.93A, 1983b, 333-336.
- [16] T.L. Bergman, R. Srinivasan, "Numerical simulation of Soret-induced double diffusion in an initially uniform concentration binary fluid", International Journal of Heat Mass Transfer, Vol.32, 1989, 679- 687.
- [17] R. Krishnan, "A numerical study of the instability of double-diffusive convection in a square enclosure with horizontal temperature and concentration gradients, heat transfer in convective flows in HTD" ASME National Heat Transfer Conference, Philadelphia, Vol.107, 1989, 357-368.

- [18] S. Rawat, R. Bhargava, "Finite element study of natural convection heat and mass transfer in a micropolar fluid-saturated porous regime with Soret/Dufour effect", *International Journal of Appl.Math. Mech.* Vol.5, 2009, 58–71.
- [19] Sunil, P. Chand, A. Mahajan and P. Sharma, "Effect of Rotation on Double-Diffusive Convection in a Magnetized Ferro fluid with Internal Angular Momentum", *Journal of Applied Fluid Mechanics*, Vol. 4(4), 2011, 43-52.
- [20] A. A. Bakr, Z. A. S. Raizahb, "Double-Diffusive Convection-Radiation Interaction on Unsteady MHD Micropolar Fluid Flow over a Vertical Moving Porous Plate with Heat Generation and Soret Effects", *Journal of Engineering and Technology*, 2012, 19-29.
- [21] R. A. Mohamed, "Double-Diffusive Convection-Radiation Interaction on Unsteady MHD Flow over a Vertical Moving Porous Plate with Heat Generation and Soret Effects", *Applied Mathematical Sciences*, Vol.3, 2009, 629-651.
- [22] A. Bahloul, N. Boutana and p. Vasseur, "Double-diffusive and Soret-induced convection in a shallow horizontal porous layer", *Journal Fluid Mech*, Vol. 491, 2003, 325–352.
- [23] Z. Alloui, H. Beji, P. Vasseur, "Double-diffusive and Soret-induced convection of a micropolar fluid in a vertical channel", *Computers and Mathematics with Applications* Vol.62, 2011, 725-736.
- [24] N. Nithyadevi, Ruey-Jen Yang, "Double diffusive natural convection in a partially heated enclosure with Soret and Dufour effects", *International Journal of Heat and Fluid Flow* Vol.30, 2009, 902–910
- [25] Ziya Uddin, Manoj Kumar, "MHD Heat and Mass Transfer Free Convection Flow Near the Lower Stagnation Point of an Isothermal Cylinder Imbedded in Porous Domain with the Presence of Radiation", *Jordan Journal of Mechanical and Industrial Engineering*, Vol. 5(2), 2011, 133 – 138.
- [26] A. Pantokratoras, "Effect of viscous dissipation in natural convection along a heated vertical plate", *Applied Mathematical Modelling* Vol. 29, 2005, 553–564.
- [27] A. K. H. Kabiri, M. A. Alim, L. S. Andallah, "Effects of Viscous Dissipation on MHD Natural Convection Flow along a Vertical Wavy Surface with Heat Generation, *American Journal of Computational Mathematics*, Vol.3, 2013, 91-98.
- [28] Osama Abu-Zeid , H. M. Duwairi, Rebhi A. Damseh, "Viscous and Joule Heating Effects over an Isothermal Cone in Saturated Porous Media, *Jordan Journal of Mechanical and Industrial Engineering*, Vol.1 (2), 2007, 113-118.
- [29] C.Y. Cheng, Fully developed natural convection heat and mass transfer of a micropolar fluid in a vertical channel with asymmetric wall temperatures and concentrations, *Int. Commun. Heat Mass Transfer* 33, 2006, 627–635.
- [30] B. S.Malga, N.Kishan, "Finite element analysis for unsteady MHD heat and mass transfer free convection flow of polar fluids past a vertical moving porous plate in a porous medium with heat generation and thermal diffusion", *Journal of Naval Architecture and Marine Engineering* Vol.11, 2014, 69-82.
- [31] B.Gebhart, "Effect of viscous dissipation in natural convection" *Journal of fluid Mechanics*, Vol.14 (2), 1962, 225-232.
- [32] S.K. Jena, M.N. Mathur, "Similarity solutions for laminar free convection flow of a thermomicropolar fluid past a nonisothermal vertical plate", *International Journal of Engrg. Science*, Vol.19, 1981, 1431-1439.
- [33] J. Peddieson, "An application of the micropolar fluid model to the calculation of a turbulent shear flow", *International Journal of Engineering Science*, Vol.10, 1972, 23-32.